Wind and Structures, Vol. 13, No. 5 (2010) 471-485
DOI: http://dx.doi.org/10.12989/was.2010.13.5.471

Study of structural parameters on the aerodynamic stability of three-tower suspension bridge

Xin-Jun Zhang*

College of Civil Engineering and Architecture, Zhejiang University of Technology, Hangzhou 310032, P.R. China

(Received August 13, 2009, Accepted May 11, 2010)

Abstract. In comparison with the common two-tower suspension bridge, due to the lack of effective longitudinal restraint of the center tower, the three-tower suspension bridge becomes a structural system with greater flexibility, and more susceptible to the wind action. By taking a three-tower suspension bridge-the Taizhou Bridge over the Yangtze River with two main spans of 1080 m as example, effects of structural parameters including the cable sag to span ratio, the side to main span ratio, the deck's dead load, the deck's bearing system, longitudinal structural form of the center tower and the cable system on the aerodynamic stability of the bridge are investigated numerically by 3D nonlinear aerodynamic stability analysis, the favorable structural system of three-tower suspension bridge with good wind stability is discussed. The results show that good aerodynamic stability can be obtained for three-tower suspension bridge as the cable sag to span ratio is assumed ranging from 1/10 to 1/11, the central buckle are provided between main cables and the deck at midpoint of main spans, the longitudinal bending stiffness of the center tower is strengthened, and the spatial cable system or double cable system is employed.

Keywords: three-tower suspension bridge; aerodynamic stability; structural parameters.

1. Introduction

Currently, the commonly built suspension bridges are two-tower structures. In the 21st century, the world's bridge construction entered into a new era of building long strait-crossing bridges. Sequential plural suspension bridges are required to cross deep straits. In such a case, each bridge must be designed with longer span to reduce the cost of the foundation and substructures. The multi-tower suspension bridge, which has no sharing anchorage, is one of the most hopeful and rational solutions (Gimsing 1997). In comparison with the common two-tower suspension bridge, the main spans of three-tower suspension bridge can be greatly shortened, as a result the tension forces in cables, the size of anchorages and foundation, and also the total cost are significantly reduced, and therefore, it becomes a competitive solution for long-span bridges.

Up to now, although there is no construction practice for three-tower suspension bridge around the world, it is proposed frequently in many long-span bridges such as the Chacao Strait Bridge in Chile, the San Francisco West Bay Bridge in America, the Messina Strait Bridge in Italy, the

* Corresponding Author, Professor, E-mail: xjzhang@zjut.edu.cn

Gibraltar Strait Bridge in Spain, the Tsugaru Strait Bridge in Japan, several highway bridges over the Yangtze River in China including the Wuhang Yangluo Bridge, the fourth Nanjing Bridge, the Maanshan Bridge and the Taizhou Bridge etc (Gimsing 1997, Forsberg and Petersen 2001, Zhu 2007). Currently, the Maanshan Bridge and the Taizhou Bridge in China, the Chacao Strait Bridge in Chile are being built as three-tower suspension bridges. On the other hand, the multi-tower suspension bridge has been recognized as a questionable structure due to its large deflection (Fukuda 1976, Gimsing 1997, Nazir 1986, Forsberg 2001). For three-tower suspension bridge, the two side towers are effectively restrained by the side cables anchored at the anchorages, however the center tower lacks of the effective longitudinal restraint, structural stiffness becomes lower than that of the common two-tower suspension bridge. In order to strengthen structural stiffness of three-tower suspension bridge, through strengthening structural stiffness of the center tower, using different cable system, and changing structural parameters etc., the static and dynamic properties of three-tower suspension bridge have been comprehensively investigated (Gimsing 1997, Yoshida *et al*. 2004, Wang 2007, Zhu 2007). As mentioned above, the three-tower suspension bridge is a structural system with greater flexibility, and becomes more susceptible to the wind action. Unfortunately until now, few investigations on the aerodynamic stability of three-tower suspension bridge have been conducted (Yoshida *et al*. 2004, Zhang 2008, Zhu 2007).

To well understand the aerodynamic stability of three-tower suspension bridge, based on the Taizhou Bridge over the Yangtze River with two main spans of 1080 m, parametric study including the cable sag to span ratio, the side to main span ratio, the deck's dead load, the deck's bearing system, longitudinal structural form of the center tower and the cable system on the aerodynamic stability of the bridge has been carried out, and the favorable structural system of three-tower suspension bridge with good wind stability is also discussed.

2. Description of the example bridge

Fig. 1(a) shows the Taizhou Highway Bridge over the Yangtze River selected as the example bridge herein, which is a three-tower suspension bridge with two 1080 m main spans and two 390 m side spans (Chen 2006). Two main cables are formed by prefabricated parallel wire strands, and spaced at 35.8 m, whose sag to span ratio is 1/9; the hangers are made of the galvanized steel wires with interval of 16 m. Fig. 1(b) shows the cross section of the bridge deck, which is a streamlined steel box girder with 3.5 m depth and 39.1 m width. The towers have a door-shaped front view, the side towers are concrete structures with an I-shaped side view, and but the center tower is a steel structure with an inverse Y-shaped side view as shown in Fig. 1(c). As compared to the side concrete towers, the steel center tower is much more slender, and can be recognized as a flexible tower. Table 1 indicates structural properties of the main cables, girder, hangers and towers.

3. Aerodynamic stability analysis of the example bridge

In the following analysis, the bridge is idealized to a 3D finite element model as shown in Fig. 2, in which the bridge deck is modeled by the single-girder model, the bridge deck and towers are modeled by 3D beam elements, and the hangers and cables are modeled by 3D bar elements, and rigid diaphragms are provided to model the connections between the bridge deck and the hangers.

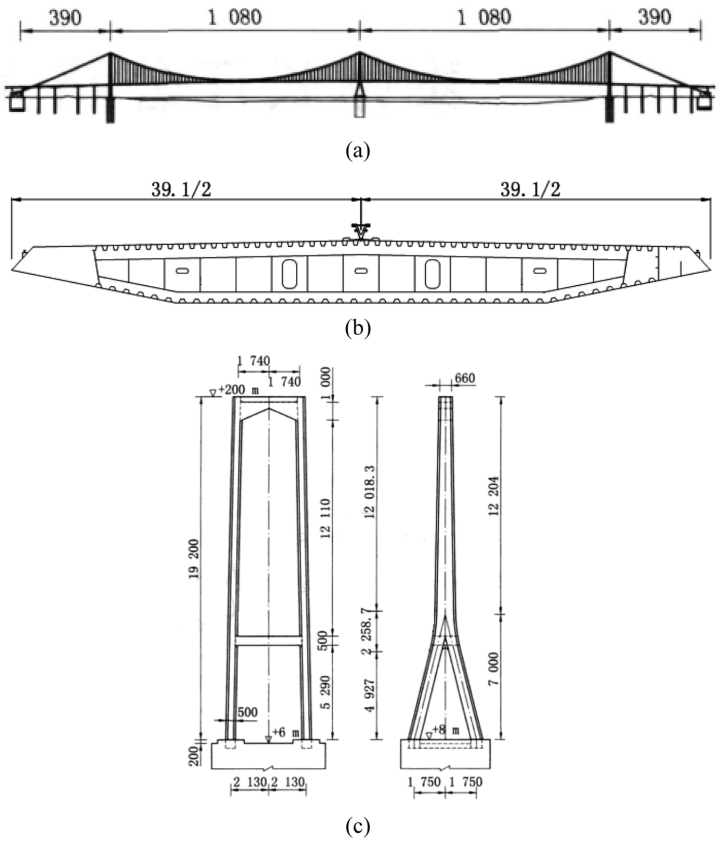

Fig. 1 (a) Side view of the Taizhou Highway Bridge over the Yangtze River (Unit: m), (b) cross section of the bridge deck (Unit: m) and (c) the center tower (Unit: mm)

Table 1 Structural properties of the Taizhou Bridge

Structural members		A/m^2	J_d/m^4	I_y/m^4	I_z/m^4	E/(MPa)	$\rho/(kg/m^3)$
Stiffening girder		1.50	8.44	192.11	2.91	2.1×10^5	13146.67
Main cable		0.286	-	-	-	2.0×10^5	7850
Hanger		0.00263	-	-	-	2.0×10^5	7850
Center tower	18*	1.556	7.261	7.203	5.599	2.1×10^5	7850
	60	3.865	29.546	94.633	14.544		
	87	3.160	16.269	32.863	10.178		
	114	3.024	14.070	25.120	9.386		
	143	2.881	11.744	18.121	8.552		
	173	1.924	7.236	8.179	5.798		
Side tower	26	38.172	568.448	442.210	284.638	3.5×10^4	2600
	105	29.56	365.321	293.219	179.918		
	186	28.381	319.278	259.788	146.461		

Note: A = cross-sectional area; J_d = torsional moment of inertia; I_y = lateral bending moment of inertia; I_z = vertical bending moment of inertia; E = elastic module; ρ = mass density; * = height of the tower's section above from the ground

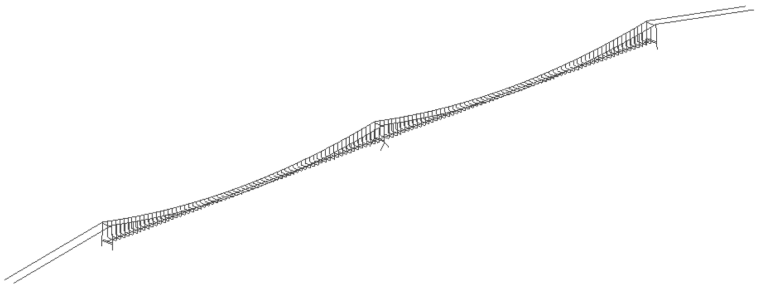

Fig. 2 3D finite element model of the example bridge

Table 2 Structural constraint conditions

Nodes	Movements and rotations					
	U_x	U_y	U_z	R_x	R_y	R_z
Towers' bottom ends	×	×	×	×	×	×
The bridge deck at side towers	⊕	×	×	×	⊕	⊕
The bridge deck at center towers	⊕	⊕	×	⊕	⊕	⊕
Cables at the anchorages	×	×	×	×	×	×

Notes: x = coordinate axis, longitudinal direction; y = coordinate axis, vertical direction; z = coordinate axis, lateral direction; U_x = movement along the x-axis; U_y = movement along the y-axis; U_z = movement along the z-axis; R_x = rotation around the x-axis; R_y = rotation around the y-axis; R_z = rotation around the z-axis; ⊕ = free; × = fixed

Structural constraint conditions are assumed as Table 2.

On the equilibrium position of the bridge in completion, the first 20 modes of the bridge are calculated by the dynamic characteristics finite element analysis (SDCA), in which the subspace iteration method is adopted and structural geometric nonlinearity is also considered (Zhang *et al*. 2002). Table 3 shows the modal properties of the bridge deck. Under wind attack angles of 0^o and $\pm 3^o$, aerodynamic stability of the bridge is investigated numerically by three-dimensional nonlinear aerodynamic stability analysis (BSNAA) (Zhang *et al*. 2002), and the critical wind speeds of aerodynamic instability are presented in Table 4. In the analysis, the bridge deck's flutter derivatives are obtained from the sectional-model wind tunnel test (Chen 2006) as plotted in Fig. 3, the first 20 modes are involved, and the modal damping ratio is taken as 0.5%.

As found in Tables 3 and 4, the computed results are very identical to those of the well known

Table 3 The modal properties of the bridge deck

Modes	Frequency (Hz)		Mode shape
	SDCA	ANSYS (Zhu 2007)	
Vertical bending	0.1155	0.1156	1-S
	0.0625	0.0769	1-AS
Lateral bending	0.0980	0.0971	1-S
	0.0733	0.0715	1-AS
Torsion	0.2523	0.2773	1-AS

Note: The number represents the modal order; S = Symmetric; AS = Anti-symmetric

Table 4 The critical wind speed of aerodynamic instability (m/s)

Wind attack angle	+3°	0°	-3°
BSNAA	59.3	79.5	73.2
Sectional-model wind tunnel test (Chen 2006)	61.9	82.8	74.2

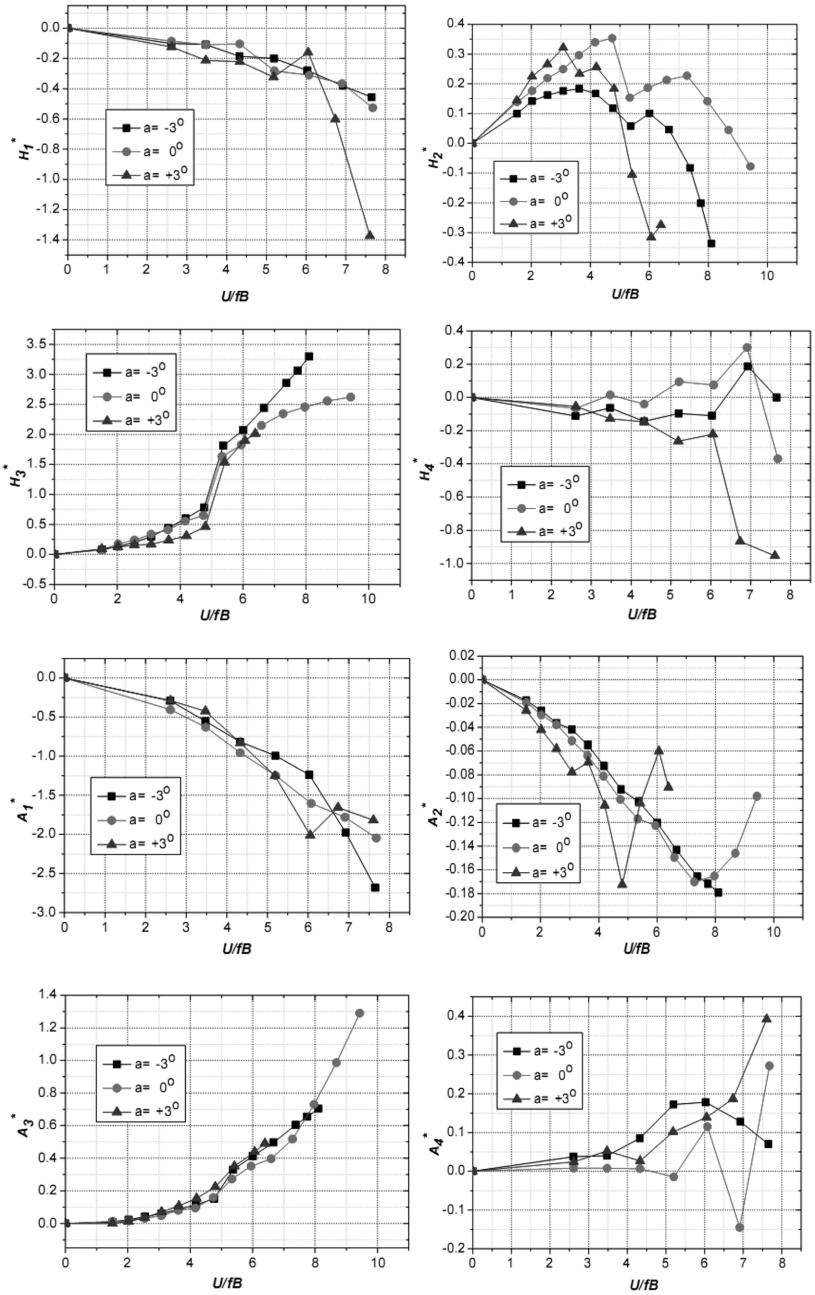

Fig. 3 Flutter derivatives at varying wind attack angles versus the reduced velocity (U/fB)

software ANSYS and the sectional-model wind tunnel test, and the validity of the employed methods is thus verified. It is also found that the aerodynamic instability of the bridge is a coupled mode dominated by the fundamental symmetric vertical bending mode and particularly the fundamental anti-symmetric torsion mode.

4. Parametric analysis

To give a guidance of wind-resistant design for three-tower suspension bridge, structural parameters including the cable sag to span ratio, the side to main span ratio, the deck's dead load, the deck's bearing system, longitudinal structural form of the center tower and the cable system are selected, their effects on the aerodynamic stability of the bridge are investigated numerically by 3D nonlinear aerodynamic stability analysis, and the favorable structural system of three-tower suspension bridges with good wind stability is also discussed.

4.1 The cable sag to span ratio

The cable sag is an important design parameter for long-span suspension bridges, which affects the tension forces in the cables and the gravity stiffness of the bridges. Generally, the cable sag to span length ratio ranges from 1/9 to 1/12 for the common two-tower suspension bridges (Gimsing 1997, Zhang and Sun 2004).

To understand how the cable sag affects the aerodynamic stability of three-tower suspension bridge, through changing the sag and corresponding structural properties of main cables, aerodynamic stability of the bridge with different cable sags is analyzed, and the critical wind speeds are given in Table 5.

As seen from Table 5, the cable sag has important influence on the critical wind speed. As the cable sag decreases, the critical wind speed increases gradually, and then decreases greatly as the cable sag to span ratio is greater than 1/11. The critical wind speed reaches to the maximum value within the range of 1/10 to 1/11. The variation of critical wind speed is very similar to that of the torsional frequency as shown in Table 6. The torsional frequencies decrease remarkably as the cable sag to span ratio is greater than 1/10, which results in the decrease of the critical wind speeds for the bridge. Although decreasing the cable sag strengthens the vertical bending stiffness, it is not aerodynamically favorable for the bridge. Therefore, the cable sag to span ratio, which ranges from 1/10 to 1/11, is favorable aerodynamically for three-tower suspension bridge.

4.2 The side span length

The side span length is also an important design parameter that affects the overall vertical bending stiffness of the common two-tower suspension bridges. As the side span length increases, the cable

Table 5 Effect of the cable sag to span ratio on the critical wind speed (m/s)

Cable sag to span ratio		1/8	1/9	1/10	1/11	1/12
Wind attack angle	+3°	58.2	59.3	59.5	64.5	56.3
	0°	79.8	79.5	81.1	80.1	68.2
	-3°	72.0	73.2	74.0	83.8	69.3

Table 6 Effect of the cable sag to span ratio on natural frequency (Hz)

Modes	Cable sag to span ratio					Mode shape
	1/8	1/9	1/10	1/11	1/12	
Vertical bending	0.1119	0.1155	0.1193	0.1231	0.1270	1-S
	0.0576	0.0625	0.0640	0.0639	0.0639	1-AS
Lateral bending	0.0966	0.0980	0.0994	0.1008	0.1021	1-S
	0.0716	0.0733	0.0750	0.0766	0.0781	1-AS
Torsion	0.3171	0.3232	0.3213	0.3098	0.2980	1-S
	0.2460	0.2523	0.2491	0.2446	0.2409	1-AS

sag in the side spans becomes large, and the cable's restraint for the center span is then weakened, which makes the center span more flexible. For the common two-tower suspension bridges, the side span to main span ratio generally ranges from 0.2 to 0.4 (Gimsing 1997, Zhang and Sun 2004).

To investigate the influence of the side span length on the aerodynamic stability of three-tower suspension bridge, remaining the main spans unchanged, aerodynamic stability of the bridge with different side span length is analyzed, and the critical wind speeds are given in Table 7.

It can be seen that the side span length has no influence on the critical wind speed. The fact can be due to almost no change of the natural frequencies as shown in Table 8. But for the common two-tower suspension bridges, the critical wind speed decreases as the side span length increases (Zhang and Sun 2004). Therefore for three-tower suspension bridges, the side span length is not a sensitive structural parameter, and can be determined by the static and economical performances.

4.3 The deck's dead load

For long-span suspension bridges, the gravity stiffness, which develops from the dead load of the cables and the deck, contributes a great deal to the overall vertical bending stiffness (Gimsing

Table 7 Effect of the side to main span ratio on the critical wind speed (m/s)

Side to main span ratio		0.2	0.25	0.3	0.35	0.4
Wind attack angle	+3°	60.1	60.1	60.1	60.1	60.1
	0°	79.5	79.5	79.6	79.6	79.6
	-3°	73.2	73.2	73.2	73.2	73.2

Table 8 Effect of the side to main span ratio on natural frequency (Hz)

Modes	Side to main span ratio					Mode shape
	0.20	0.25	0.30	0.35	0.40	
Vertical bending	0.1156	0.1156	0.1155	0.1155	0.1155	1-S
	0.0625	0.0625	0.0625	0.0625	0.0625	1-AS
Lateral bending	0.0980	0.0980	0.0980	0.0980	0.0980	1-S
	0.0734	0.0734	0.0733	0.0733	0.0733	1-AS
Torsion	0.3237	0.3234	0.3233	0.3233	0.3232	1-S
	0.2521	0.2522	0.2523	0.2523	0.2523	1-AS

Table 9 Effect of the deck's dead load on the critical wind speed (m/s)

Dead load ratio		1	1.2	1.4
Wind attack angle	+3°	59.3	59.0	59.3
	0°	79.5	69.5	67.7
	-3°	73.2	73.8	74.5

Table 10 Effect of the deck's dead load on natural frequency (Hz)

Modes	Dead load ratio			Mode shape
	1.0	1.2	1.4	
Vertical bending	0.1155	0.1152	0.1150	1-S
	0.0625	0.0604	0.0586	1-AS
Lateral bending	0.0980	0.0925	0.0880	1-S
	0.0733	0.0701	0.0676	1-AS
Torsion	0.3232	0.3127	0.3063	1-S
	0.2523	0.2403	0.2301	1-AS

1997). With increasing of the deck's dead load, the tension forces in the cables increase, and the vertical bending stiffness of the bridge is thus strengthened. In order to investigate how the deck's dead load affects the aerodynamic stability of three-tower suspension bridge, aerodynamic stability of the bridge with different deck's dead load is analyzed, and the critical wind speeds are given in Table 9.

As seen in Table 9, the critical wind speed decreases with increasing of the deck's dead load. It can be attributed to the decrease of the torsional frequencies as shown in Table 10. Increasing the deck's dead load adds structural mass, to a certain extent, the strengthening of the vertical bending stiffness is counteract by the increase of mass, the vertical bending frequency decreases slightly, whereas the torsional frequency decreases significantly. On the other hand, adding the deck's dead load will lead to an uneconomical design. Therefore, it is by no means an effective measure to improve the aerodynamic stability for the bridge by increasing the deck's dead load.

4.4 The deck's bearing system

For the example bridge, the deck floats longitudinally, which is favorable to earthquake resistance for the bridge. However, under certain loading conditions, large longitudinal displacement happens. The central buckle and longitudinal elastic cable used to limit the large longitudinal displacement, have been adopted in several long-span suspension bridges (Chen and Zhong 2008, Ji and Zhong 2006). To investigate the effect of the deck's bearing system on the aerodynamic stability of the bridge, remaining other structural parameters the same as the example bridge, three cases are assumed: for case 1, the longitudinal elastic cables are provided between the deck and the center tower to restrain the deck's longitudinal displacement; for case 2, the central buckles are provided at the midpoints of two main spans; for case 3, both the longitudinal elastic cables and central buckles are provided. Aerodynamic stability of the bridge with different deck's bearing systems is analyzed, and the critical wind speeds are given in Table 11.

As seen in Table 11, the critical wind speed is basically not influenced by the longitudinal elastic

Table 11 Effect of the deck's bearing system on the critical wind speed (m/s)

The girder's bearing system		Floating system*	Longitudinal elastic cables	Central buckles	Longitudinal elastic cables and central buckles
Wind attack angle	+3°	59.3	60.1	67.0	67.0
	0°	79.5	79.6	89.9	89.9
	-3°	73.2	73.2	83.0	83.0

Note: *=the example bridge

Table 12 Effect of the deck's bearing system on natural frequency (Hz)

Modes	The deck's bearing system				Mode shape
	Floating system	Longitudinal elastic cables	Central buckles	Longitudinal elastic cables and central buckles	
Vertical bending	0.1155	0.1159	0.1525	0.1534	1-S
	0.0625	0.0716	0.0732	0.0737	1-AS
Lateral bending	0.0980	0.0980	0.0990	0.0990	1-S
	0.0733	0.0741	0.0740	0.0747	1-AS
Torsion	0.3232	0.3230	0.3562	0.3562	1-S
	0.2523	0.2523	0.2764	0.2765	1-AS

cables, and however it is increased by 13% in the case of the central buckle used. The fact can be attributed to the increase of natural frequencies as given in Table 12. Therefore, the central buckle is confirmed analytically to be favorable aerodynamically for the bridge.

4.5 Cable system

Commonly, the suspension bridge has two parallel cable planes, and in each cable plane there is only one main cable, which is named as parallel single cable system herein. In order to get greater structural stiffness of three-tower suspension bridge, several investigations on the favorable cable system have been conducted, and the spatial cable system and the double cable system are believed to be favorable for three-tower suspension bridge with respect to structural static and dynamic properties (Astiz 1998, Gimsing 1997, Yoshida *et al*. 2004, Zhu 2007, Lin *et al*. 2007). To investigate the effect of cable system on the aerodynamic stability of the bridge, two case bridges are designed, one with spatial cable system and another with double cable system.

Fig. 4 shows the 3D finite element model of the case bridge with spatial cable system. The distance of two main cables is reduced to as narrow as possible at the tower top and gradually expanded towards the midpoint of the main span by the transverse component of the hangers' tension. All three towers are A-shaped in front view. The cable sag to span ratio is 1/9 in elevation, and 17.9/1080 in plane, the geometric shape of the cables is both parabola in elevation and plane. Except the cables, other structural parameters are remained the same as those of the example bridge.

Fig. 5 shows the 3D finite element model of the case bridge with double cable system. There are two main cables with different sags in each cable plane, and the upper and bottom cables are

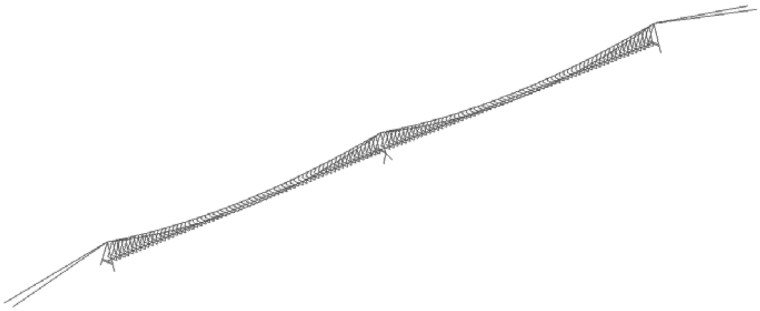

Fig. 4 3D finite element model of the case bridge with spatial cable system

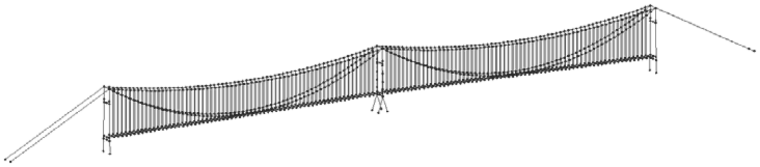

Fig. 5 3D finite element model of the case bridge with double cable system

connected with the vertical hangers. The sag to span ratio is 1/20 for the upper main cable, and 3/20 for the bottom main cable, the geometric shapes of the upper and bottom cables are both parabola. The height of the midpoints of the bottom cables is the same as the example bridges. In determining the cables' cross-sectional areas, 20% of the deck's dead load is acted on the upper cables, and for the bottom cables, 80% of the deck's dead load is acted, the safety factors are assumed to be 2.7 and 2.5 for the upper and bottom cables respectively, and the design tensile strength of cable material is 1670 MPa. Under such assumptions, the calculated cross-sectional areas of the upper and bottom cables are 0.1776 m^2 and 0.1804 m^2 respectively, and the total cross-sectional area is 25% greater than that of the example bridge. Except the cables and towers, other structural parameters are remained the same as those of the example bridge.

4.5.1 Dynamic characteristics

On the equilibrium position of the above case bridges in completion, the first 20 modes are calculated, and in Table 13, the modal properties of the bridge deck are shown.

In the case of spatial cable system, the vertical bending frequencies do not change basically, and the lateral bending frequencies increase slightly, and but the first anti-symmetric torsional frequency has a great increase as compared to the example bridge. It means that the lateral bending and particular torsional stiffness is strengthened importantly by introducing three-dimensional cable system, which is also confirmed by previous static performance investigations (Astiz 1998, Gimsing 1997, Yoshida *et al.* 2004, Wang 2007, Zhu 2007).

In the case of double cable system, as compared to the example bridge, the vertical bending frequencies have a remarkable increase, and but the lateral bending frequencies almost do not change. It means that the vertical bending stiffness is strengthened with adopting the double cable system, which is also demonstrated by the previous studies (Gimsing 1997, Wang 2007, Zhu 2007, Lin *et al*. 2007). With the strengthening of structural vertical bending stiffness, the torsional frequency increases consequently.

Table 13 Effect of cable system on natural frequency (Hz)

Modes	Cable system			Mode shape
	Parallel single cable system*	Spatial cable system	Double cable system	
Vertical bending	0.1155	0.1151	0.1593	1-S
	0.0625	0.0623	0.1816	1-AS
Lateral bending	0.0980	0.0994	0.0976	1-S
	0.0733	0.0752	0. 0703	1-AS
Torsion	0.2523	0.3775	0.2775	1-AS
	0.3232	0.3336	0.3255	1-S

Note: *=the example bridge

It can be concluded that better dynamic characteristics is obtained by adopting the spatial and double cable system for three-tower suspension bridge, which is proved to be favorable aerodynamically as described follows.

4.5.2 Aerodynamic stability

Under aerodynamic attack angles of 0^o and $\pm 3^o$, aerodynamic stability of the above case bridges is analyzed, and the critical wind speeds are presented in Table 14.

As found in Table 14, in comparison with the example bridge, the critical wind speeds increase significantly as the double and especially spatial cable systems are adopted. In the case of double cable system, the critical wind speed is more than 6% higher that of the example bridge, and in the case of spatial cable system, the critical wind speed is more than 30% higher that of the example bridge. The significant increase of the critical wind speed can be attributed to the greater torsional frequencies obtained as shown in Table 13. Therefore, adopting either the spatial or double cable system is confirmed analytically to be an effective structural solution to improve the aerodynamic stability of three-tower suspension bridge, and the spatial cable system seems to be more favorable aerodynamically.

4.6 Longitudinal structural form of the center tower

The center tower structure has important influence on the mechanical behavior of a three-tower suspension bridge such as the deflection of main span and the slip resistance between the main cable and saddle on the center tower etc. Different longitudinal structural form of the center tower gives different longitudinal bending stiffness, the longitudinal I, A and inversed Y-shaped structural forms of the center tower have been investigated with respected to the static behavior (Gimsing 1997, Ruan *et*

Table 14 Effect of cable system on the critical wind speed (m/s)

Cable system		Parallel single cable system	Spatial cable system	Double cable system
Wind attack angle	$+3^o$	59.3	81.6	64.6
	0^o	79.5	109.9	84.6
	-3^o	73.2	98	78.8

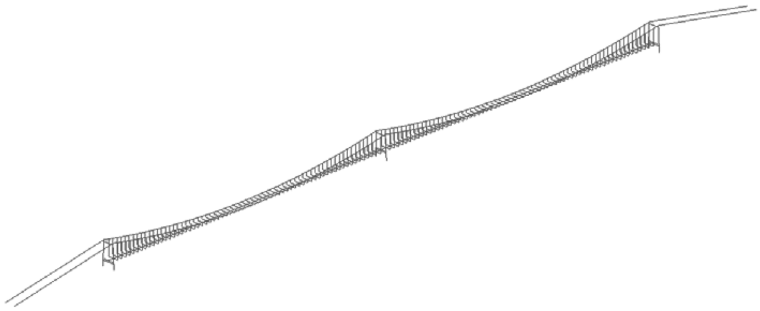

Fig. 6 3D finite element model of the case bridge with a concrete longitudinal I-shaped center tower

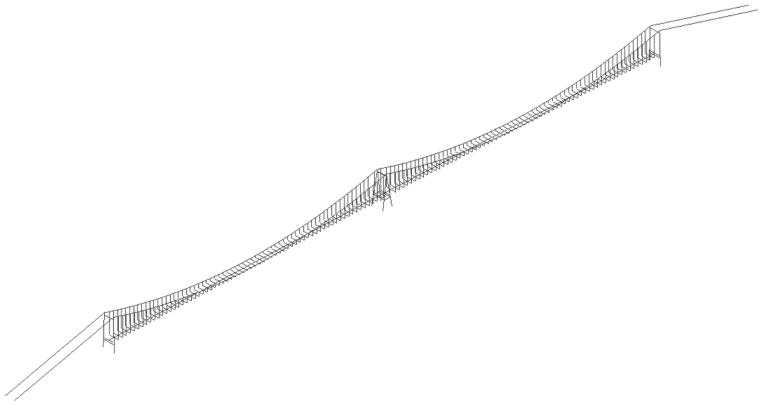

Fig. 7 3D finite element model of the case bridge with a concrete longitudinal A-shaped center tower

al. 2008). To investigate the longitudinal bending stiffness of the center tower on the aerodynamic stability of the bridge, remaining the other structural parameters unchanged, three case bridges are designed by changing the longitudinal structural form of the center tower: case bridge 1 has a concrete longitudinal I-shaped center tower as shown in Fig. 6, and its material and cross-sectional properties are the same as the side towers; case bridge 2 has a concrete longitudinal A-shaped center tower as shown in Fig. 7; case bridge 3 has a concrete longitudinal inversed Y-shaped center tower.

4.6.1 Dynamic characteristics

On the equilibrium position of the above case bridges in completion, the first 20 modes are analyzed, and the modal properties of the bridge deck are given in Table 15.

As the concrete center tower is adopted, in comparison with the example bridge with steel center tower, the first anti-symmetric vertical bending frequency and particularly the first anti-symmetric torsional frequency have a remarkable increase. Instead of steel center tower, as known from Table 1, structural stiffness of the center tower is remarkably strengthened as concrete center tower is adopted. For the anti-symmetric vertical bending and torsion modes, the center tower bends longitudinally and twists itself. Due to the significant stiffening of longitudinal bending stiffness of the center tower, the anti-symmetric vertical bending and particularly torsional frequencies therefore increase greatly.

In addition, under the same concrete center tower, due to the further stiffening of longitudinal bending stiffness of the center tower, the anti-symmetric vertical bending and torsional frequencies

Table 15 Effect of longitudinal structural form of the center tower on natural frequnecy (Hz)

Modes	Center tower				Mode shape
	Steel inversed Y-shaped*	Concrete I-shaped	Concrete A-shaped	Concrete inversed Y-shaped	
Vertical bending	0.1155	0.1155	0.1157	0.1155	1-S
	0.0625	0.0669	0.0875	0.0739	1-AS
Lateral bending	0.0980	0.0992	0.0996	0.0990	1-S
	0.0733	0.0733	0.0733	0.0733	1-AS
Torsion	0.2523	0.3046	0.3079	0.3095	1-AS
	0.3232	0.3261	0.3352	0.3620	1-S

Note: *=the example bridge

of the bridges with longitudinal A-shaped and inversed Y-shaped center tower increase further as compared to the bridge with longitudinal I-shaped center tower.

4.6.2 Aerodynamic stability

Under aerodynamic attack angles of 0° and +3°, aerodynamic stability of the above case bridges is analyzed, and the critical wind speeds of aerodynamic instability are presented in Table 16.

In comparison with the example bridge with steel center tower, the critical wind speed in the case of concrete center tower has a remarkable increase. The fact can be mainly attributed to the increase of the anti-symmetric torsional frequency as shown in Table 15. Under the same concrete center tower, due to the further increase of the anti-symmetric torsional frequency, the critical wind speeds of the bridges with longitudinal A-shaped and inversed Y-shaped center tower increase further as compared to the bridge with longitudinal I-shaped center tower. Therefore, strengthening longitudinal bending stiffness of the center tower is confirmed analytically to be favorable aerodynamically for three-tower suspension bridge.

5. Conclusions

In this work, by taking a three-tower suspension bridge-the Taizhou Highway Bridge over Yangtze River with two main spans of 1080 m as example, effects of structural parameters including the cable sag to span ratio, the side to main span ratio, the deck's dead load, the deck's bearing system, longitudinal structural form of the center tower and the cable system on the aerodynamic stability of the bridge are investigated numerically by 3D nonlinear aerodynamic stability analysis, and some important conclusions are drawn as follows:

(1) The cable sag to span ratio, which ranges from 1/10 to 1/11, is favorable aerodynamically for

Table 16 Effect of longitudinal structural form of the center tower on the critical wind speed (m/s)

Center tower		Steel inversed Y-shaped*	Concrete I-shaped	Concrete A-shaped	Concrete inversed Y-shaped
Wind attack angle	+3°	59.3	72.9	70.1	73.8
	0°	79.5	88.5	99.0	89.6

three-tower suspension bridge.

(2) The side span length has no influence on the aerodynamic stability of three-tower suspension bridge.

(3) Adding the deck's dead load can not improve the aerodynamic stability of three-tower suspension bridge.

(4) The central buckles at the midpoints of main spans are favorable aerodynamically for three-tower suspension bridge.

(5) Stiffening the longitudinal bending stiffness of the center tower is effective in improving the aerodynamic stability of three-tower suspension bridge.

(6) Using the spatial and double cable systems is an effective structural solution to improve the aerodynamic stability of three-tower suspension bridge, and the spatial cable system seems more favorable aerodynamically.

Acknowledgements

The writers would like to thank to Zhejiang Provincial Science Foundation of China for their financial support. The flutter derivatives employed in this paper are obtained from the wind tunnel results provided by Tongji University, the writers also appreciate Prof. A.R. Chen, and the State Key Laboratory for Disaster Reduction in Civil Engineering of Tongji University for their kind support.

References

Astiz, M.A. (1998), "Flutter stability of very long suspension bridges", *J. Bridge Eng.*, **3**(3), 132-139.

Chen, A.R. (2006), *Aerodynamic-resistant Research on the Taizhou Highway Bridge over the Yangtze River: sectional-model aerodynamic tunnel test*, Research Report, the State Key Laboratory for Disaster Reduction in Civil Engineering, Tongji University.

Chen, C. and Zhong, J.C. (2008), "Impact of key design parameters of three-tower suspension bridge on structural behavior of the bridge", *World Bridges*, **2**, 10-12.

Forsberg, T. (2001), "Multi-span suspension bridges", *Int. J. Steel Struct.*, **1**(1), 63-73.

Forsberg, T. and Petersen, A. (2001), "The challenge of constructing a bridge over the Chacao channel", *Proceedings of the IABSE conference on Cable-supported bridges-challenging technical limits*, Seoul, Korea.

Fukuda, T. (1976), "Analysis of multispan suspension bridges", *J. Struct. Div.,* **94**, 63-86.

Gimsing, N.J. (1997), *Cable-supported bridges - concept & design*, 2nd Edition, John Wiley & Sons Ltd., England.

Ji, L. and Zhong, J. (2006), "Runyang suspension bridge over the Yangtze River", *Struct. Eng. Int.*, **3**, 194-199.

Lin, L.X., Wu, Y.P. and Ding, N.H. (2007), "Influence of structure parameters on natural vibration characteristics of double-cable suspension bridge", *J. China Rail. Soc.*, **29**(4), 91-95.

Nazir, C.P. (1986), "Multispan balanced suspension bridge", *J. Struct. Eng.*, **112**(11), 2512-2527.

Ruan, J., Ji, L. and Zhu, J.P. (2008), "Structure style selection of the mid-tower of a three-tower suspension bridge", *J. Shandong Univ. (Engineering Science)*, **38**(2), 106-111.

Wang, P. (2007), *Static and dynamic characteristics of multi-tower continuous suspension bridges*, Dissertation of Southwest Jiaotong University, China.

Yoshida, O., Okuda, M. and Moriya, T. (2004), "Structural characteristics and applicability of four-span suspension bridge", *J. Bridge Eng.*, **9**(5), 453-463.

Zhang, X.J., Xiang, H.F. and Sun, B.N. (2002), "Nonlinear aerostatic and aerodynamic analysis of long-span suspension bridges considering wind-structure interactions", *J. Wind. Eng. Ind. Aerod.*, **90**(9), 1065-1080.

Zhang, X.J. (2008), "Wind stability of three-tower suspension bridges", *Wind Struct.,* **11**(4), 341-344.
Zhang, X.J. and Sun, B.N. (2004), "Parametric study on the aerodynamic stability of a long-span suspension bridge", *J. Wind Eng. Ind. Aerod*., **92**(6), 431-439.
Zhu, B.J. (2007), *Structural system research of multi-tower suspension bridge*, Dissertation of Tongji University, China.

CC